03

The use of thermoelectric detector in gas ionized by a shock wave

© M.A. Kotov[1,2], P.V. Kozlov[2], V.Yu. Levashov[2], G.Ya. Gerasimov[2], N.G. Solovyov[1], A.N. Shemyakin[1], M.Yu. Yakimov[1], V.N. Glebov[3], G.A. Dubrova[3], A.M. Malyutin[3]

[1] Ishlinsky Institute for Problems in Mechanics, Russian Academy of Sciences, Moscow, Russia
[2] Institute of Mechanics of Lomonosov Moscow State University, Moscow, Russia
[3] Institute of Laser and Information Technologies–Shatura, Kurchatov Complex of Crystallography and Photonics, NRC „Kurchatov Institute," Shatura, Moscow oblast, Russia
E-mail: kotov@ipmnet.ru

Received February 18, 2025
Revised March 26, 2025
Accepted March 26, 2025

The aspects of operation of a thermoelectric detector in a shock-heated partially ionized air environment are considered. The effect of charged particles located near its sensitive element on the detector readings is shown. Data on the registration of the photoionization process before the shock wave front are presented.

Keywords: shock tube, thermoelectric detector, ionization.

DOI: 10.61011/TPL.2025.06.61303.20289

The study of processes proceeding near the surface of a lander moving in the atmosphere of the Earth and other planets of the Solar System is particularly relevant to the development of the rocket and space industry [1,2]. Various kinds of installations, including shock tubes, are used for ground-based modeling of conditions established when shock-heated gas flows around spacecraft. Shock tubes make it possible to achieve high values of enthalpy of the incoming gas flow, but the characteristic time of such processes is limited to several tens of microseconds. Special thermoelectric detectors (TD), which generate thermal EMF under thermal load, may be used to measure heat fluxes under such conditions. Most of them are fitted with sensitive elements made of electrically conductive materials. Their readings may be influenced by charged particles that are produced in shock-heated gas as a result of ionization processes. The design of various TD types and the generation of the thermal load signal were discussed in detail in [3].

It should be noted that TDs yield fairly correct results of measurement of heat fluxes when the degree of gas ionization is low. Specifically, a detector of this kind was used to record the ignition of a propane–air mixture behind a reflected shock wave at a shock-heated gas temperature up to 1700 K and a pressure up to 20 atm and above [3]. The heat flux intensities reported in these measurements reached $7\,\mathrm{MW/m^2}$ within $0.5\,\mu\mathrm{s}$; the origins of the rise fronts in the corresponding time dependences matched the pressure sensor readings.

In partially ionized gases, the interpretation of data obtained using certain TD types may be ambiguous. This is evidenced by experiments on measurement of the heat flux behind a reflected shock wave in xenon with a significant degree of ionization, where certain signal features indicating the influence of charged particles were observed [4]. The present study is focused on the analysis of data obtained using a TD in partially ionized air, the characterization of influence of charged particles on its readings, and the investigation of its applicability in monitoring of ionization processes before and behind the front of a strong shock wave (SW).

Experiments were carried out in a double-diaphragm shock tube. Its operating principle was detailed in [5]. A shock wave was formed in the air-filled low-pressure chamber (LPC) with an internal circular cross section 57 mm in diameter. Electric probes Z1 and Z2 for plasma parameter recording had a single-electrode design and were positioned along the direction of propagation of the shock wave. The electrodes protruded by approximately 1 mm into the working part of the LPC (the protrusion could vary slightly in size, since it was difficult to monitor its dimensions in the LPC after installing the probe); their diameter was 0.4 mm. The electrode material was stainless steel AISI 304. A TD with a sensitive element based on chromium crystallites was mounted between the electrodes flush with the inner wall of the LPC. Its readings were recorded through an analog-to-digital converter with a sampling frequency of 2.5 MHz per channel. The diagram of the experiment with the positioning and dimensions of the measurement devices indicated is presented in Fig. 1.

The circles with minuses in Fig. 1 show schematically the regions of electrons formed near Z1, TD, and Z2 as a result of photoionization. The TD width was 5 mm (photograph above the diagram in Fig. 1, *a*); measuring instruments Z1, TD, and Z2 had no external electric potential.

The emission of shock-heated gas behind the front of a strong SW with a photon energy exceeding the ionization energy of gas molecules spreads into the region of undisturbed gas before the SW and is absorbed partially by the layer closest to the SW front, which leads to its photoionization ($N_2 + h\nu \rightarrow N_2^+ + e^-$ and $O_2 + h\nu \rightarrow O_2^+ + e^-$) [5].

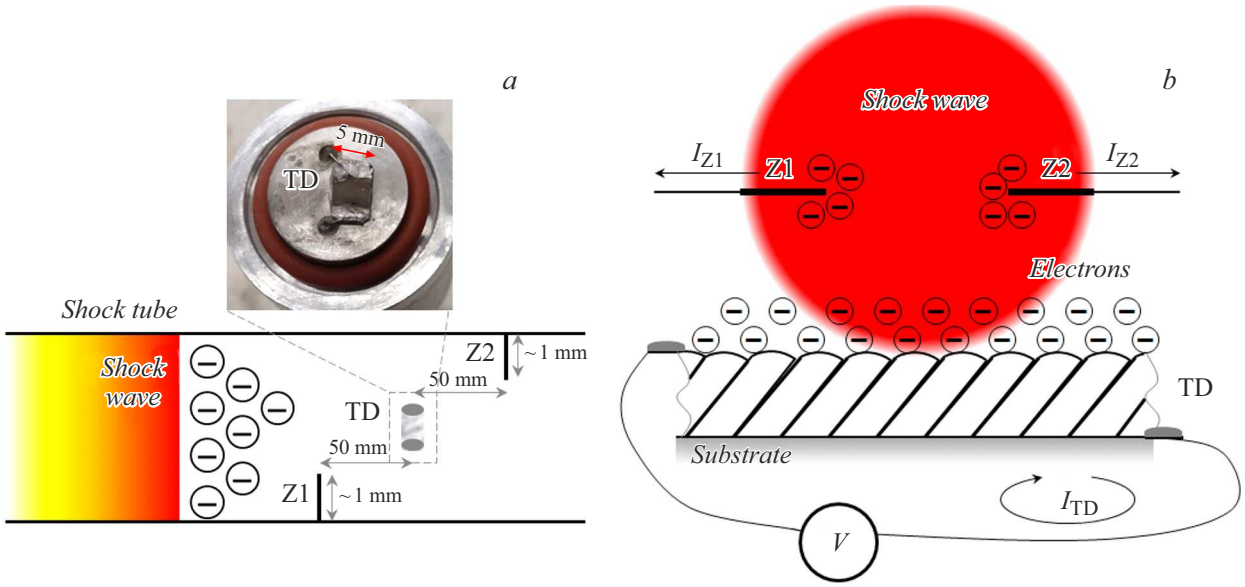

Figure 1. Positioning of probes (Z1, Z2) and the thermoelectric detector (TD) in the shock tube LPC. *a* — Side view; *b* — front view (facing the shock wave).

The production of electrons and their subsequent thermal movement to the surface of Z1, TD, and Z2 induce currents I_{Z1}, I_{TD} and I_{Z2}. The sensitive layer of the used TD is a system of heteraxial chromium crystallites arranged on a high-resistance substrate via vacuum deposition at an oblique condensation angle (Fig. 1, *b*). The EMF is measured through contact pads located on the sensor substrate. Just as in single-electrode probes, a directed movement of charged particles in a closed circuit forms in such a structure when a negative potential is applied to the upper plane (the electron concentration increases). A charge difference between the upper (additional electrons formed before the SW) and lower planes induces current I_{TD}.

Figure 2 shows the time dependences of readings of probes Z1 and Z2 and the TD detector within the time interval from -140 to $0\,\mu$s, where the zero point coincides with the arrival of the shock front at the TD detector. The initial pressure in the LPC is 0.25 Torr, and the SW front velocity is 9.86 km/s. The readings of Z1 and Z2 at large distances from the SW reveal the influence of the photoelectric effect from radiation of shock-heated gas, which gives way to photoionization immediately before the arrival of the SW front.

The electron work function for the surface of stainless steel from which the probes are fabricated is estimated at 3.5 eV and above [6], which is equivalent to the energy of photons at a wavelength of 354 nm and below. With these parameters, the temperature of the most heated part of non-equilibrium air plasma behind the SW front may be estimated approximately at 10 kK [7]. The spectrum of such plasma features both several typical bands in the UV region and continuum emission characterized by Planck's law [5]. The spectral radiance of plasma is sufficient to knock out electrons from the surface of electrodes of the probes and increase their potentials (Fig. 2, Z1: from -140 to $-50\,\mu$s; Z2: from -110 to $20\,\mu$s). The emission of heated plasma with an energy exceeding the ionization energy of air particles before the SW front is partially absorbed by the air layer closest to the SW front, which leads to its ionization, and partially spreads further and ionizes gas regions increasingly distant from the SW front. Owing to thermal motion, electrons reach the surface of probes Z1 and Z2, reducing their positive potential and eventually making this potential negative (Fig. 2, Z1: from $-50\,\mu$s onwards; Z2: from $-20\,\mu$s onwards). Since the intensity of transmitted radiation decreases exponentially with increasing layer thickness, the concentration of electrons is the highest near the SW front.

The contribution of photoionization processes is immediately evident in the TD readings (Fig. 2, TD: from $-130\,\mu$s onwards), since the photoelectric effect is non-existent here due to the planar design of the sensor and its placement flush with the LPC wall (Fig. 1). This approach provides an opportunity to determine more accurately the region of onset of photoionization before the SW.

The SW emission characteristics were also measured. The radiation level recorded through the side window within the wavelength range of 200–300 nm (i.e., at energies allowing for the observation of the photoelectric effect [5]) more than $1\,\mu$s before the SW arrival at the TD measurement section is 3–4 orders of magnitude lower than the maximum one, which is also indicative of a lack of the photoelectric effect. Data on the measurement of emission of the SW front and the assessment of its curvature were reported in [8]. These data suggest that with the process parameters examined in the study, the SW front may be considered sufficiently stable

and flat and local instabilities before the SW front may be neglected.

Figure 2 allows one to determine the moment of time $t = -100\,\mu$s after which the influence of charged particles on the TD readings becomes evident, indicating the onset of photoionization before the SW front (at a velocity of 9.86 km/s). The electron concentration was estimated under similar experimental conditions in [5,9,10]; its values 1000 mm ahead of the SW front are on the order of $N_e = 10^{10}-10^{11}$ cm^{-3}. It is fair to assume that this electron concentration is a certain threshold value above which the influence of charged particles on the TD readings needs to be taken into account.

The passage of the SW front observed through the TD readings is slower (Fig. 3). This is attributable to the size of the measurement area of its sensitive element (5 mm versus a diameter of 0.4 mm of the Z1 and Z2 electrodes, Fig. 1, *a*) around which the concentration of positively charged particles increases gradually. The time of passage of the SW front through this measurement area is slightly shorter than 5 μs at an SW velocity of 9.86 km/s (the region between the dashed lines in Fig. 3). The TD readings feature fluctuations after a sharp rise. In addition to charged particles, these fluctuations are affected by the thermal EMF generated by the TD due to convective and radiative heating from gas behind the SW [11]. It is rather difficult to determine experimentally the ionization parameters of gas behind the SW front, since plasma is highly non-equilibrium and several competing processes are present: ionization and recombination, vibrational-translational relaxation, local thermodynamic equilibration, and transient gas-dynamic processes of heat and mass transfer caused by mixing of hot masses [1,2].

The presented results indicate that the sensitive element of the used thermoelectric detector responds to the concentration of charged particles near it. The potential of the sensor may change not only due to the generation of thermal EMF by the incoming heat flux, but also under the influence of electrons located nearby. This aspect must be taken into account when one operates a thermoelectric detector in ionized gases. The potential for use of thermoelectric detectors to record ionization processes in shock-wave interactions (e.g., to examine the region where the photoionization process starts before the front of strong SWs) is also noteworthy. The discussed method may be of use in ground-based shock-tube tests simulating the entry of spacecraft into dense layers of the atmospheres of planets and satellites of the Solar System. Data obtained in such tests may be compared with the readings of ionization sensors that are mounted on actual spacecraft and record the distributions of charged particles in the course of the flight and descent [12,13].

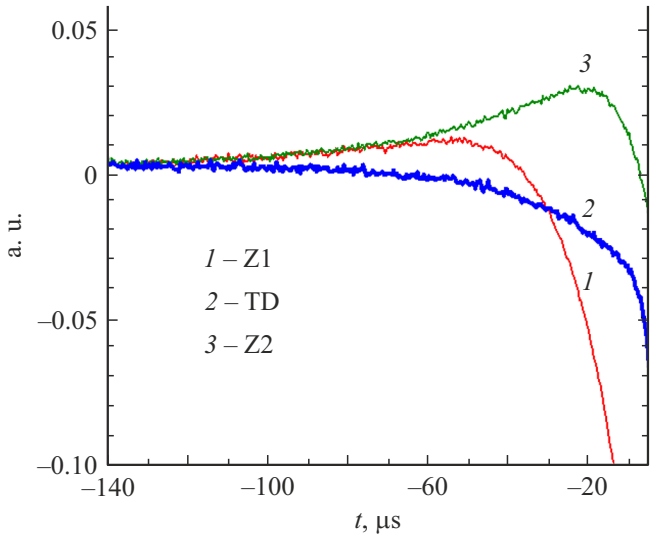

Figure 2. Signals from probes Z1, Z2 and the thermoelectric detector revealing the photoelectric effect and photoionization before the shock wave.

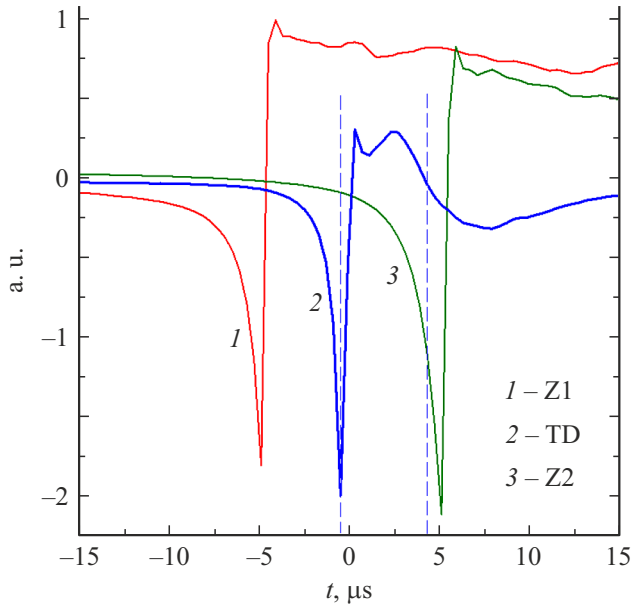

Figure 3. Comparison of Z1, Z2, and TD readings during the passage of the shock wave front.

Acknowledgments

The authors wish to thank P.A. Popov for the idea underlying this work.

Funding

This study was carried out under the state assignment of the Moscow State University, the Ministry of Science and Higher Education of the Russian Federation (state registration number 124012500440-9), and the state assignment of the National Research Center „Kurchatov Institute."

Conflict of interest

The authors declare that they have no conflict of interest.

References

[1] Ya.B. Zel'dovich, Yu.P. Raizer, *Physics of shock waves and high-temperature hydrodynamic phenomena* (Dover Publ., 2002).
[2] S.T. Surzhikov, *Komp'yuternaya aerofizika spuskaemykh kosmicheskikh apparatov. Dvukhmernye modeli* (Fizmatlit, M., 2018) (in Russian). https://www.rfbr.ru/library/books/2521/
[3] M.A. Kotov, N.G. Solovyov, A.N. Shemyakin, M.Yu. Yakimov, V.N. Glebov, G.A. Dubrova, A.M. Malyutin, P.A. Popov, S.A. Poniaev, T.A. Lapushkina, V.A. Sakharov, P.V. Kozlov, V. Yu Levashov, G.Ya Gerasimov, Fiz.-Khim. Kinet. Gazov. Din., **25**, 3 (2024) (in Russian). DOI: 10.33257/PhChGD.25.3.1114
[4] M.A. Kotov, A.N. Shemyakin, N.G. Solovyov, M.Yu. Yakimov, V.N. Glebov, G.A. Dubrova, A.M. Malyutin, P.A. Popov, S.A. Poniaev, T.A. Lapushkina, N.A. Monakhov, V.A. Sakharov, J. Phys.: Conf. Ser., **2103**, 012218 (2021). DOI: 10.1088/1742-6596/2103/1/012218
[5] M.A. Kotov, P.V. Kozlov, G.Ya Gerasimov, V. Yu Levashov, K.Yu. Osipenko, N.G. Bykova, I.E. Zabelinsky, Acta Astron., **217**, 130 (2024). DOI: 10.1016/j.actaastro.2024.01.035
[6] R. Wilson, J. Appl. Phys., **37**, 3170 (1966). DOI: 10.1063/1.1703180
[7] P.V. Kozlov, N.G. Bykova, G. Ya Gerasimov, V. Yu Levashov, M.A. Kotov, I.E. Zabelinsky, Acta Astron., **214**, 303 (2024). DOI: 10.1016/j.actaastro.2023.10.033
[8] T. Morioka, N. Sakurai, K. Maeno, H. Honma, J. Visualization, **3** (1), 51 (2000). DOI: 10.1007/BF03182440
[9] M. Omura, L.L. Presley, AIAA J., **7** (12), 2363 (1969). DOI: 10.2514/3.5554
[10] S. Nomura, T. Kawakami, K. Fujita, J. Thermophys. Heat Transfer, **35** (3), 518 (2021). DOI: 10.2514/1.T6057
[11] F.V. Filippov, M.A. Kotov, N.G. Solovyov, V.N. Glebov, G.A. Dubrova, A.M. Malyutin, Tech. Phys. Lett., **50** (12), 45 (2024). DOI: 10.61011/TPL.2024.12.60349.6591k.
[12] A. Gülhan, T. Thiele, F. Siebe, R. Kronen, T. Schleutker, J. Spacecraft Rockets, **56** (1), 68 (2019). DOI: 10.2514/1.A34228
[13] S.T. Surzhikov, D.S. Yatsukhno, Fluid Dyn., **57** (6), 768 (2022). DOI: 10.1134/S0015462822600924.

Translated by D.Safin